

Abstract

19
20
21
22
23
24
25
26
27
28
29
30
31
32
33
34
35
36
37
38
39
40
41
42
43

G-protein gated inwardly rectifying K^+ (GIRK) channels are the major inwardly rectifying K^+ currents in cardiac atrial myocytes and an important determinant of atrial electrophysiology. Inhibitory G-protein alpha subunits can both mediate activation via acetylcholine but can also suppress basal currents in the absence of agonist. We studied this phenomenon using whole cell patch clamping in murine atria from mice with global genetic deletion of $G\alpha_{i2}$, combined deletion of $G\alpha_{i1}/G\alpha_{i3}$ and littermate controls. We found that mice with deletion of $G\alpha_{i2}$ had increased basal and agonist activated currents particularly in the right atria whilst in contrast those with $G\alpha_{i1}/G\alpha_{i3}$ deletion had reduced currents. Mice with global genetic deletion of $G\alpha_{i2}$ had decreased action potential duration. Tissue preparations of the left atria studied with a multielectrode array from $G\alpha_{i2}$ knockout mice showed a shorter effective refractory period, with no change in conduction velocity, than littermate controls. Transcriptional studies revealed increased expression of GIRK channel subunit genes in $G\alpha_{i2}$ knockout mice. Thus different G-protein isoforms have differential effects on GIRK channel behaviour and paradoxically $G\alpha_{i2}$ acts to increase basal and agonist activated GIRK currents. Deletion of $G\alpha_{i2}$ is potentially proarrhythmic in the atria.

Keywords: atria, electrophysiology, inhibitory heterotrimeric G-protein, G-protein gated potassium channel

Running Title: Inhibitory G-proteins and atrial electrophysiology

Abbreviations: GIRK G protein-dependent inwardly rectifying potassium, Kir potassium inwardly rectifying channel, SA node sinoatrial node, LA left atria, RA right atria, RNA

44 ribonucleic acid, BSA bovine serum albumine, HEPES 4-(2-Hydroxyethyl)piperazine-1-
45 ethanesulfonic acid, N-(2-Hydroxyethyl)piperazine-N'-(2-ethanesulfonic acid), MEA multi-
46 electrode array, CV conduction velocity, AERP atrial effective refractory period, kcnj5 G
47 protein-activated inward rectifier potassium channel 4 gene, Gnai1 Guanine nucleotide-
48 binding protein G(i), alpha-1 subunit gene, Gnai3 Guanine nucleotide-binding protein G(i)
49 gene, alpha-3 subunit gene, Gnb1 Guanine nucleotide-binding protein subunit beta-1 gene,
50 Gnb4 Guanine nucleotide-binding protein subunit beta-4 gene, Gng11 Guanine nucleotide-
51 binding protein subunit gama-11 gene, Gng7 Guanine nucleotide-binding protein subunit
52 gama-7 gene, GAPDH glyceraldehyde-3-phosphate dehydrogenase.

53

Introduction

54

55

56 Inwardly rectifying K⁺ channels are widely expressed in all chambers of the heart and
57 are important in setting the resting membrane potential. However there is a dichotomy with
58 the Kir2.0 family being predominant in the ventricles and His-Purkinje system and the Kir3.0
59 family in atrial and nodal tissues (7; 18; 24; 45). The Kir3.0 channel family encodes G-
60 protein gated inwardly rectifying K⁺ channel present in neurons and neuroendocrine tissues
61 in addition to the heart (11; 27). In the heart the channel is thought to consist largely of a
62 heteromultimer of Kir3.1 and Kir3.4 (19). A characteristic of these channels is that they are
63 activated by G-protein coupled receptors linked to inhibitory G-proteins and specifically by
64 the free Gβγ subunits (25; 42; 44). For example, in the sinoatrial node activation of the
65 channel by acetylcholine released from the vagus nerve is responsible for heart rate slowing
66 (39; 43). Recently a study has shown a critical role for Kir3.4 in the kinetics of heart rate
67 recovery to resting level after sympathetic activation (30).

68 Despite GIRK channel activation being mediated by Gβγ directly binding to domains
69 on the channel, activation seems to occur largely via members of the inhibitory G-protein
70 family (14; 21; 22; 35). In a series of studies from different laboratories using varied
71 approaches a more complex model has emerged. It appears that the inhibitory G-protein
72 heterotrimer is able to directly interact with channel and on activation heterotrimer
73 dissociation occurs in a microdomain in or around the channel subunit. The dissociated Gβγ
74 subunit leads to activation (9; 21; 34; 38). However the Gα as either a monomer or as part of
75 the heterotrimer may also play an important role leading to inhibition of channel activity and
76 this process may be isoform dependent (5; 6; 15). Multiple isoforms of inhibitory Gα
77 subunits (Gα_{i1}, Gα_{i2}, Gα_{i3} and, Gα_o) are present in atrial tissue, and their roles in modulating

78 parasympathetic signal transduction remain unclear. The subunits $G\alpha_{i2}$, $G\alpha_{i3}$ have been
79 shown to mediate signaling to GIRK in embryonic stem cell derived cardiomyocytes (Sowell
80 et al., 1997). Our own work shows that $G\alpha_{i2}$ is important for heart rate regulation *in-vivo* (41;
81 46) but this occurs via modulation in the SA node (not the atria) and might be via a
82 mechanism independent of GIRK.

83 There is further complexity in that the right and left atria may be different and have
84 gradients of channel expression (17). GIRK channels are expressed at higher levels in the
85 right atrium in mice and humans. It has been proposed that the gradient of GIRK current,
86 combined with the heterogenous distribution of parasympathetic innervation and adenosine
87 receptor expression in the atria, may contribute to the ability of vagal nerve stimulation to
88 augment dispersion of atrial refractoriness (12; 13; 23; 26; 40). The purpose of this study is to
89 define the type of G-proteins involved in the signalling to GIRK in the atria, the possible role
90 of these G-proteins in atrial asymmetry and how they might potentially modulate
91 arrhythmogenesis.

92

93

Material and Methods

94 *Gene-targeted mice*

95 Mice with global deletion of $G\alpha_{i2}$, and $G\alpha_{i1}/G\alpha_{i3}$ (deletion of both $G\alpha_{i1}$ and $G\alpha_{i3}$)
96 maintained on a Sv129 background were compared with wild-type littermate controls. The
97 gene-targeting strategy, genotyping and confirmation of relevant $G\alpha_{i/o}$ deletions have
98 previously been described (16; 46). Mice were maintained in an animal core facility under the
99 UK Home Office guidelines relating to animal welfare. All procedures were approved by the
100 local animal care and use committee and performed in accord with the UK Home Office
101 regulations (PPL 70\7665). All mice were kept in a temperature controlled environment (21-
102 24°C) with 12/12hr light/dark cycle. Animals were allowed ad-libitum access to standard
103 rodent chow and drinking water. Mice on a 129/Sv background aged 3–4 months (20-30 g)
104 were used for this study. Both males and females were used in the study and there was no
105 gender discrimination. Littermate controls were obtained from the $G\alpha_{i2}$ crosses.

106

107 *Quantitative real time reverse transcription PCR*

108 RNA was isolated from the left atria and right atria from 14 week old mice with
109 global deletion of $G\alpha_{i2}$ (n=3), maintained on a Sv129 background and wild-type littermate
110 controls (n=3) using the RNeasy kit (Qiagen). Briefly, hearts were removed from each group
111 of mice ($G\alpha_{i2}$ (+/+) and, $G\alpha_{i2}$ (-/-)), washed with cold PBS, left atria and right atria were
112 isolated and immediately placed in RNA Later. RNA was extracted using RNeasy kit (cat no.
113 74104 Qiagen). cDNA was synthesized using the High capacity cDNA reverse transcription
114 Kit (4368814 Life technologies) quantified and 50ng of cDNA/20 μ l was used for the
115 subsequent real time expression assay. Real-time PCR was performed using Taqman gene
116 expression Assays (Life technologies). All genes (Mm00434618_m1: Kcnj3,

117 Mm01175829_m1: Kcnj5, Mm00492379_m1: Gnai3, Mm01165301_m1: Gnai1,
118 Mm00494677_m1: Gnb1, Mm00501973_m1: Gnb4, Mm01165191_m1: Gng11,
119 Mm00515876_m1: Gng7) were assayed in triplicates and GAPDH was used as the house
120 keeping gene.

121

122 *Single-cell isolation and electrophysiology*

123 Atrial and sinoatrial cells were isolated using an adapted method for isolation of
124 sinoatrial cardiomyocytes (29). Briefly, mice were injected with heparin and beating hearts
125 were removed under pentobarbital (3 ml/kg) and ketamine (1 ml/kg) anaesthesia. The left and
126 right atria were excised in normal Tyrode solution containing (mM): NaCl, 140; KCl, 5.4;
127 CaCl₂, 1.8; MgCl₂, 1; HEPES–NaOH, 5; and D-glucose, 5.5; (pH 7.4). Strips of tissues were
128 enzymatically digested in a low-Ca²⁺ and low- Mg²⁺ solution containing (mM): NaCl, 140;
129 KCl, 5.4; MgCl₂, 0.5; CaCl₂, 0.2; KH₂PO₄, 1.2; taurine, 50; D-glucose, 5.5; HEPES–NaOH,
130 5; pH 6.9. Collagenase type II (224 U/ml, Worthington), elastase (1.9 U/ml, Worthington),
131 protease (0.9 U/ml, Sigma Aldrich), and bovine serum albumin (BSA) 1 mg/ml were added.
132 The digestion step was carried out for 20 min or 45 min, for atrial and SAN tissue,
133 respectively, under gentle mechanical agitation at 37°C. Tissue strips were then washed out,
134 and transferred into a modified ‘Kraftbrühe’ (KB) medium containing (mM): l-glutamic acid,
135 70; KCl, 20; KOH, 80; d-β-OH-butyric acid, 10; KH₂PO₄, 10; taurine, 10; BSA, 1 mg/ml;
136 and HEPES–KOH, 10; pH 7.4. Single myocytes were manually dissociated in KB solution by
137 employing a fire-polished glass pipette. Finally, extracellular Ca²⁺ concentration was
138 recovered up to 1.3 mM. A drop of cell suspension was seeded onto sterilised laminin-coated
139 coverslips. After 30-45 min, Tyrode solution containing 10% BSA was added, and cells were
140 stored at 37°C until used in humidified 5% CO₂-95% air at 37⁰C. All experiments were
141 performed at room temperature.

142 Patch-clamp current recordings were performed with an Axopatch 200B amplifier
143 (Axon Instruments) using fire-polished pipettes with a resistance of 3-4 M Ω pulled from
144 filamented borosilicated glass capillaries (Harvard Apparatus, 1.5 mm OD x 1.17 mm ID).
145 Data were acquired and analysed by using a Digidata 1322A interface (Axon Instruments)
146 and pCLAMP software (version 10, Axon Instruments). Action potentials were recorded in
147 the current clamp mode. Cardiomyocytes were stimulated using a 5 ms current pulse. The
148 resting membrane potential, the magnitude of the initial depolarisation and the action
149 potential duration at which 50 and 90% repolarisation occurred were measured (APD₅₀ and
150 APD₉₀ respectively). The cells were clamped at -60 mV in an extracellular solution
151 containing (mM): NaCl 135, KCl 5.4, CaCl₂ 2, MgCl₂ 1, NaH₂PO₄ 0.33, H-HEPES 5,
152 Glucose 10 (buffered to pH 7.4 with NaOH). The intracellular solution was (mM): K
153 gluconate 110, KCl 20, NaCl 10, MgCl₂ 1, MgATP 2, EGTA 2, Na₂GTP 0.3 (buffered to pH
154 7.2 with KOH). The liquid junction potential was +13 mV.

155

156 *Measurement of atrial electrophysiology using multielectrode arrays*

157 Using a multi-electrode array (MEA, Multichannel Systems), we investigated the
158 effect of ablation of G α_{i2} on electrophysiological parameters in ex-vivo atrial tissue (33). Left
159 atria were dissected from isolated mouse hearts after mounting in a Langendorff setup and
160 perfused with Krebs solution supplemented with 30 mM 2, 3-butanedione monoxime. The
161 tissue was then transferred to the array perfused with Krebs solution (37°C; 95% O₂ / 5%
162 CO₂). Experiments were conducted in the absence and the presence of 10 nM – 10 μ M
163 carbachol. Left atrial electrophysiology was assessed during electrical stimulation using a
164 multi-electrode array (MEA) system which allows non-invasive synchronous multifocal
165 recording of extracellular field potentials. The MEA (MEA2100, Multichannel Systems,
166 Reutlingen, Germany) consists of 60 microelectrodes arranged in an 8 \times 8 matrix, with a 20

167 μm electrode diameter and an inter-electrode distance of 200 μm , Myocardial samples were
168 positioned in the center of the MEA dish, held in contact with electrodes by a holder, and
169 continuously superfused with oxygenated Krebs solution at 37°C. Baseline electrical
170 stimulation (bipolar pulses, 2x threshold, 2ms duration, 4 Hz frequency) was applied via one
171 of the MEA microelectrodes. Field potential data were acquired simultaneously from all 60
172 microelectrodes. S1-S2 train stimulation with a S1-S1 cycle length of 250 ms was used to
173 assess atrial effective refractory period (AERP). To assess conduction properties, isolated
174 atria were sequentially stimulated (4 Hz) from one electrode of each 4 edges of the array.
175 Field potential recordings obtained in these conditions were processed using LabChart7
176 (ADINSTRUMENTS, UK) to define local activation time based on minimum of the
177 derivative of field potential. Average conduction velocity (CV) was calculated by linear
178 regression relating inter electrode distance to activation times, as previously described (Opel
179 et al., 2015). The slope of the regression line was the average conduction velocity (CV).
180 Minimal wave-front cycle length (WFCL) was calculated for each isolated atria as AERP x
181 CV.

182

183 *Statistical Analysis*

184 The mean and standard error of the mean are presented. Student's t-test or one way
185 ANOVA was used, with a *P*-value < 0.05 being statistically significant.

186

Results

Inward currents in right and left atria

Using a step voltage protocol, current-voltage (I-V) relationships of atrial cardiomyocytes isolated from the right atria (RA) and left atria (LA) were compared in control mice (normal genotype littermates from the $G\alpha_{i2}$ crosses) (Figure 1). Currents were larger and showed greater inward rectification in RA than in the LA in the presence of carbachol (Figure 1 and 3). Experiments were also performed in the presence of $GTP\gamma S$ in the patch pipette to activate GIRK currents in the absence of receptor stimulation. In these experimental conditions, we still obtained a larger current in RA (-59.8 ± 6.5 pA/pF, $n=5$) compared to LA (-27.8 ± 2 pA/pF, $n=5$) of $G\alpha_{i2}$ (+/+) atrial myocytes ($n=5$ mice).

In $G\alpha_{i2}$ (-/-) mice, the I/V relationship of the RA was altered with larger basal and carbachol-activated inward currents in the RA (Figure 2 and 4). In mice with the combined deletion of $G\alpha_{i1}/G\alpha_{i3}$ there were reduced carbachol-activated currents in the RA (Figure 3 and 4). The effects of $G\alpha_{i2}$ deletion were more pronounced in the RA, leading to loss of regional difference across the atria. Kinetics of GIRK current activation by carbachol were assessed using a twenty second application of agonist as we have previously described (2; 3; 31). There were no major changes in activation and rapid desensitisation between RA and LA and in the mice with either $G\alpha_{i2}$ or $G\alpha_{i1}/G\alpha_{i3}$ deletion (Table 1). In contrast, deactivation was slower in the RA than the LA but this pattern was not changed in the $G\alpha_{i2}$ (-/-) mice and in mice with combined $G\alpha_{i1}/G\alpha_{i3}$ deletion (Table 1).

We examined for expression changes of relevant components in the signalling cascade in the RA and LA of $G\alpha_{i2}$ (-/-) mice and littermate controls. Using quantitative real time reverse transcription PCR, we measured the expression of $G\alpha_{i1}$ (Gnai1), $G\alpha_{i3}$ (Gnai3),

211 some representative Gβγs (Gnb1, Gnb4, Gng7, Gng11) and the GIRK channel subunits (Kcnj3
212 and Kcnj5) and the results are shown in Table 2. Gnb4 and Gng11 were chosen as they have
213 potentially been associated with cardiovascular traits in particular heart rate in genome wide
214 association studies (10). In general, the changes between $G\alpha_{i2}$ (-/-) mice and littermate
215 controls are modest even when significant. However in $G\alpha_{i2}$ (-/-) mice GIRK channel subunit
216 kcnj5 expression was increased in both atrial chambers suggesting that some of the
217 differences in regulation of GIRK channels in $G\alpha_{i2}$ (-/-) mice may be related to
218 transcriptional changes in channel expression.

219

220 *Comparison with the SA node*

221 We also isolated and patch clamped SA nodal cells. GIRK currents were of a similar
222 magnitude as that in the RA but rectified more strongly and deactivated more rapidly after
223 carbachol application (Figure 5 and Table 1). The properties of the currents in the SA node
224 were unaffected in mice with global genetic deletion of $G\alpha_{i2}$ or $G\alpha_{i1}/G\alpha_{i3}$.

225

226 *Single-cell action potentials*

227 It might be predicted that an increased GIRK current in $G\alpha_{i2}$ (-/-) mice might lead to a
228 shortened action potential duration and atrial effective refractory period. We compared atrial
229 action potentials in the RA and LA myocytes in control and $G\alpha_{i2}$ (-/-) mice and, found that
230 RA atrial myocytes from RA $G\alpha_{i2}$ (-/-) mice had a shorter APD₉₀ than control RA myocytes.
231 A similar trend was observed in the LA myocytes though this was not statistically significant
232 (Figure 6).

233 Carbachol (10μM) led to shortening of APD with a more pronounced effect in the
234 RA. The decrease of the APD₉₀ reached 61 ± 3 % in $G\alpha_{i2}$ (+/+) LA (n=9, n=3 mice) and $76 \pm$

235 3 % in $G\alpha_{i2}$ (+/+) RA (n= 8, n=3 mice, p=0.006). In $G\alpha_{i2}$ (-/-) murine atrial myocytes,
236 carbachol decreased APD_{90} by $57 \pm 7\%$ in the LA (n=7, n=3 mice) and by $50 \pm 8\%$ in the RA
237 (n=6, n=3 mice, NS).

238

239 *Tissue electrophysiology*

240 We performed an analysis of the tissue electrophysiology in isolated left atria using a
241 multielectrode array. The analysis of intact right atria was complicated by the intrinsic
242 pacemaking activity. In the $G\alpha_{i2}$ (-/-) LA, there was a shortened effective refractory period
243 (ERP), and no alteration in conduction velocity in comparison to $G\alpha_{i2}$ (+/+) LA, resulting in
244 a significant decrease in potential path length for re-entry (Figure 7). A similar relative
245 decrease of left atrial ERP was observed in the presence of carbachol (10 nM to 10 μ M)
246 between $G\alpha_{i2}$ (-/-) and control, with no significant difference in log EC_{50} , i.e. -6.9 ± 0.4 vs -
247 7.1 ± 0.4 respectively. Carbachol did not alter left atrial CV (Figure 7, n=7).

248

249

Discussion

250
251
252
253
254
255
256
257
258
259
260
261
262
263
264
265
266
267
268
269
270
271
272
273
274

Our main findings are that in murine atria specific isoforms of inhibitory G-proteins have defined roles in controlling GIRK channel function. Specifically $G\alpha_{i2}$ suppresses the basal and agonist induced activity of GIRK whilst $G\alpha_{i1}$ and/or $G\alpha_{i3}$ mediate muscarinic activation of the current. Our experiments are in agreement with previous work, showing larger GIRK currents in the RA and the SAN regions compared to the LA region (12; 13; 23; 26; 40). Deletion of $G\alpha_{i2}$ accentuated this chamber asymmetry whilst it was attenuated in mice with global genetic deletion of $G\alpha_{i1}$ and $G\alpha_{i3}$. In keeping with the changes in GIRK currents, the global genetic deletion of $G\alpha_{i2}$ resulted in a shortened action potential duration, reduced tissue atrial effective refractory period and reduced minimum wave front cycle length.

These findings complement our previous work in which we have investigated heart rate regulation in various G-protein alpha subunit knockout mice (41; 46). Specifically mice with global and SA node specific deletion of $G\alpha_{i2}$ were tachycardic with impaired high frequency responses in heart rate variability studies. It is worth stating that the majority of studies reported here were conducted in the atria and reveal differences between the SA node and across the atria in GIRK channel signalling and G-protein dependency. Our observations reported here in the SA node show preserved signalling via muscarinic receptors to GIRK channels with deletion of both $G\alpha_{i2}$ and combined $G\alpha_{i1}\backslash G\alpha_{i3}$. This suggests that GIRK channel independent mechanisms may be important in determining the *in-vivo* phenotype in $G\alpha_{i2}$ knockout mice. Specifically the loss of negative coupling to adenylate cyclase, fall in cAMP and effects on the hyperpolarization activated cyclic nucleotide gated channel and/or modulation of protein kinase A regulating the “calcium clock” may be important (20).

275 *Inhibitory G-protein α subunits and GIRK channel function*

276 GIRK channels are traditionally viewed as an example of a canonical effector
277 activated by $G\beta\gamma$ subunits. However it is clear that $G\alpha$ subunits play a role. For example, we
278 demonstrated in heterologous systems that channel activation seemed to be preferentially
279 activated via inhibitory rather than stimulatory G-proteins (21). Furthermore, studies have
280 shown that the inhibitory G-protein heterotrimer can bind to the channel complex (6; 9; 37).
281 This interaction may have important functional consequences namely that it suppresses basal
282 current activity (6; 34). In other studies the Dascal laboratory demonstrated that there may be
283 isoform differences in the nature of this behaviour between $G\alpha_{i1}$ and $G\alpha_{i3}$ (15). One issue
284 with a proportion of this work is that the conclusions often depend on overexpression of
285 engineered components in heterologous expression systems. It is unclear whether these kinds
286 of effect occur in native settings with physiological levels of G-protein and channel
287 expression. In this study in native atrial myocytes we show that deletion of $G\alpha_{i2}$ leads to an
288 unexpected increase in basal and agonist activated currents. One interpretation of this finding
289 is that inhibitory G-protein α subunits do indeed have an ability in-vivo to negatively regulate
290 GIRK currents. However, our data reveal another potential mechanism namely transcriptional
291 changes in GIRK channel subunit expression engendered by $G\alpha_{i2}$ deletion. Specifically in the
292 $G\alpha_{i2}$ (-/-) mice, expression levels for *kcnj3* and *kcnj5* mRNA, in a statistically significant
293 fashion for the latter, were increased compared to littermate controls and the magnitude of
294 these effects were comparable to the changes in GIRK current density observed. In contrast,
295 combined deletion of $G\alpha_{i1}$ and $G\alpha_{i3}$ impairs the magnitude of muscarinic activation
296 suggesting that one of $G\alpha_{i1}$ and $G\alpha_{i3}$ or both is important for mediating the agonist induced
297 response. Although we studied single isolated cardiac cells *ex-vivo*, it is still possible that
298 extracardiac effects could lead to long lasting changes in myocyte biology.

299 We also examined if deletion of $G\alpha_{i2}$ had effects on the expression of other
300 components in the signalling cascade namely $Gnai1$, $Gnai3$, $Gnb1$, $Gnb4$, $Gng7$ and $Gng11$.
301 These experiments have substantial practical complications as there are five G-protein beta
302 genes and fourteen G-protein gamma genes. We selected four to examine for compensatory
303 changes in part determined from genome wide association studies in heart rate and our own
304 unpublished studies (10). Whilst there were some changes these were modest in magnitude
305 (possible decreases in expression of $gnb1$ and $gng11$ in the LA but no significant change
306 change in $gnb4$, $gng7$, $gnai1$ or $gnai3$). Furthermore, in the functional studies in $G\alpha_{i2}$ (-/-)
307 mice, carbachol led to increased agonist induced current activation suggesting $G_{\beta\gamma}$ expression
308 was not limiting for signal transduction.

309

310 *Regional differences*

311 There were regional differences in the nature and coupling profile of GIRK currents
312 in supraventricular tissues. GIRK currents were larger in the right atrium and SA node and
313 these differences were accentuated in the right atrium by global genetic deletion of $G\alpha_{i2}$.
314 Kinetic analysis also showed that GIRK current inactivation is faster in the RA and the SAN
315 regions compared to the left atrium. This fast inactivation of the GIRK currents in the RA and
316 pacemaker regions could reflect differential expression of regulators of G-protein signalling
317 that can increase the hydrolysis rate of GTP bound and active G-protein α subunits (4; 33;
318 36). Furthermore, GIRK currents were more outwardly rectifying in the SA node and this
319 could contribute to their importance in recovery of heart rate after exercise as explored
320 recently in GIRK4 knockout mice as they may play a more significant role at depolarised
321 potentials (30).

322 Another interesting finding is that the molecular details of the signalling system differ
323 between closely related regions of the heart. So whilst $G\alpha_{i2}$ and $G\alpha_{i1}$ / $G\alpha_{i3}$ seem to have roles

324 in inhibition and activation respectively in the atria this pattern does not exist in the SA node.
325 Indeed, a significant amount of redundancy is suggested as GIRK channel activation was
326 little affected in both $G\alpha_{i2}$ and $G\alpha_{i1}\backslash G\alpha_{i3}$ knockout mice. This suggests that the specifics of
327 the signalling can be tissue and region dependent. G-protein deletion had no effect on the
328 kinetics of signalling suggesting that this was predominantly determined by other factors such
329 as the expression of regulators of G-protein signalling.

330

331 *G-protein deletion and predisposition to arrhythmia*

332 The increase in GIRK currents in mice with global genetic deletion of $G\alpha_{i2}$ might
333 lead to more general effects on single cell and tissue level electrophysiology. Indeed, the
334 increase GIRK currents was sufficient to decrease the action potential duration. Furthermore,
335 in whole left atrial preparations, $G\alpha_{i2}$ shortened the atrial effective refractory period without
336 an effect on conduction velocity leading to a decrease minimum wave front cycle length. This
337 change would be potentially proarrhythmic. We have also previously observed that $G\alpha_{i2}$
338 deletion in the ventricle and silencing of the vagal input increases the predisposition to
339 ventricular arrhythmia (28; 47). The mechanism is different with an effect on calcium
340 channel regulation and expression (47). It is also known that GIRK4 knockout mice are
341 resistant to the induction of atrial fibrillation whilst RGS6 knockout mice with increased
342 GIRK channel activity are predisposed (18; 36). Other investigators have observed in the dog
343 that $G\alpha_{i2}$ and/or $G\alpha_{i3}$ knockdown using cell permeable peptides may suppress vagally
344 mediated atrial fibrillation when delivered into the posterior left atrium (1). The authors did
345 not examine the specifics of the mechanism and whether it was related to GIRK channel
346 activation.

347 Action potential duration has been shown to decrease with increasing distance from
348 the SAN region (26; 32). In contrast, GIRK currents are larger in the right atrium than left

349 atrium and this suggests there are other important electrophysiological determinants of the
350 variation in action potential duration across the atria. The shortened action potential duration
351 in the left atrium is potentially important as it may allow the support of higher frequency
352 rotors in and around the pulmonary veins (40) though in this study the authors found higher
353 GIRK currents in the left versus right atrium of sheep. Despite this lack of consensus,
354 suppression of GIRK channel activity in the left atrium abrogates re-entry and atrial
355 fibrillation (8).

356

357 *Conclusions*

358 Whilst not directly addressing the issue our studies are compatible with the long
359 standing view that $G\beta\gamma$ subunits are important for GIRK channel activation. However they do
360 reveal layers of complexity in how the $G\alpha$ heterotrimeric G-protein subunit might shape this
361 response. A body of work, which we discuss above, has suggested various ways by which
362 this might occur including direct protein-protein interaction between G-protein heterotrimer
363 components and channels domains. However much of this work is accomplished by
364 expressing components, often at non-physiological levels, in model cell systems. Here we
365 examine native signalling in various chambers and regions of the heart using mice with
366 global genetic deletion of $G\alpha$ subunits. Our overall conclusion is that there is much plasticity
367 in the system with the exact importance of a specific $G\alpha$ subunit being dependent on tissue
368 region expression. $G\alpha$ subunits may directly suppress GIRK currents in native systems but
369 this could be accounted for by additional effects on channel transcription. These observed
370 phenomena may result from variations in $G\alpha$ subunit expression or compartmentation with
371 the channel in different cardiac regions and these are topics for future investigation.

372

373 *Acknowledgements*

374 We thank the British Heart Foundation (RG/15/15/31742) and the Intramural
375 Research Program of the NIH (project Z01ES101643) for funding this research. D.M. was
376 supported by a grant from la Fédération Française de Cardiologie. The authors have no
377 conflicts of interest to declare.

378

379

Reference List

380
381
382
383
384
385
386
387
388
389
390
391
392
393
394
395
396
397
398
399

1. **Aistrup GL, Villuendas R, Ng J, Gilchrist A, Lynch TW, Gordon D, Cokic I, Mottl S, Zhou R, Dean DA, Wasserstrom JA, Goldberger JJ, Kadish AH and Arora R.** Targeted G-protein inhibition as a novel approach to decrease vagal atrial fibrillation by selective parasympathetic attenuation. *Cardiovasc Res* 83: 481-492, 2009.
2. **Benians A, Leaney JL, Milligan G and Tinker A.** The dynamics of formation and action of the ternary complex revealed in living cells using a G-protein-gated K⁺ channel as a biosensor. *J Biol Chem* 278: 10851-10858, 2003.
3. **Benians A, Leaney JL and Tinker A.** Agonist unbinding from receptor dictates the nature of deactivation kinetics of G-protein gated K⁺ channels. *Proc Natl Acad Sci U S A* 100: 6239-6244, 2003.
4. **Benians A, Nobles M, Hosny S and Tinker A.** Regulators of G-protein signalling form a quaternary complex with the agonist, receptor and G-protein: a novel explanation for the acceleration of signalling activation kinetics. *J Biol Chem* 280: 13383-13394, 2005.
5. **Berlin S, Keren-Raifman T, Castel R, Rubinstein M, Dessauer CW, Ivanina T and Dascal N.** G α (i) and G β gamma jointly regulate the conformations of a G β gamma effector, the neuronal G protein-activated K⁺ channel (GIRK). *J Biol Chem* 285: 6179-6185, 2010.

- 400 6. **Berlin S, Tsemakhovich VA, Castel R, Ivanina T, Dessauer CW, Keren-Raifman T**
401 **and Dascal N.** Two distinct aspects of coupling between Galpha(i) protein and G
402 protein-activated K⁺ channel (GIRK) revealed by fluorescently labeled Galpha(i3)
403 protein subunits. *J Biol Chem* 286: 33223-33235, 2011.
- 404 7. **Bettahi I, Marker CL, Roman MI and Wickman K.** Contribution of the Kir3.1
405 subunit to the muscarinic-gated atrial potassium channel IKACH. *J Biol Chem* 277:
406 48282-48288, 2002.
- 407 8. **Bingen BO, Neshati Z, Askar SF, Kazbanov IV, Ypey DL, Panfilov AV, Schaliy**
408 **MJ, de Vries AA and Pijnappels DA.** Atrium-specific Kir3.x determines inducibility,
409 dynamics, and termination of fibrillation by regulating restitution-driven alternans.
410 *Circulation* 128: 2732-2744, 2013.
- 411 9. **Clancy SM, Fowler CE, Finley M, Suen KF, Arrabit C, Berton F, Kosaza T, Casey**
412 **PJ and Slesinger PA.** Pertussis-toxin-sensitive Galpha subunits selectively bind to C-
413 terminal domain of neuronal GIRK channels: evidence for a heterotrimeric G-protein-
414 channel complex. *Mol Cell Neurosci* 28: 375-389, 2005.
- 415 10. **den Hoed M, Eijgelsheim M, Esko T, Brundel BJ, Peal DS, Evans DM, Nolte IM,**
416 **Segre AV, Holm H, Handsaker RE, Westra HJ, Johnson T, Isaacs A, Yang J,**
417 **Lundby A, Zhao JH, Kim YJ, Go MJ, Almgren P, Bochud M, Boucher G, Cornelis**
418 **MC, Gudbjartsson D, Hadley D, van der Harst P, Hayward C, den HM, Igl W,**
419 **Jackson AU, Kutalik Z, Luan J, Kemp JP, Kristiansson K, Ladenvall C,**
420 **Lorentzon M, Montasser ME, Njajou OT, O'Reilly PF, Padmanabhan S, St PB,**
421 **Rankinen T, Salo P, Tanaka T, Timpson NJ, Vitart V, Waite L, Wheeler W,**

422 Zhang W, Draisma HH, Feitosa MF, Kerr KF, Lind PA, Mihailov E, Onland-
423 Moret NC, Song C, Weedon MN, Xie W, Yengo L, Absher D, Albert CM, Alonso
424 A, Arking DE, de Bakker PI, Balkau B, Barlassina C, Benaglio P, Bis JC, Bouatia-
425 Naji N, Brage S, Chanock SJ, Chines PS, Chung M, Darbar D, Dina C, Dorr M,
426 Elliott P, Felix SB, Fischer K, Fuchsberger C, de Geus EJ, Goyette P, Gudnason V,
427 Harris TB, Hartikainen AL, Havulinna AS, Heckbert SR, Hicks AA, Hofman A,
428 Holewijn S, Hoogstra-Berends F, Hottenga JJ, Jensen MK, Johansson A, Junttila
429 J, Kaab S, Kanon B, Ketkar S, Khaw KT, Knowles JW, Kooner AS, Kors JA,
430 Kumari M, Milani L, Laiho P, Lakatta EG, Langenberg C, Leusink M, Liu Y,
431 Luben RN, Lunetta KL, Lynch SN, Markus MR, Marques-Vidal P, Mateo L, I,
432 McArdle WL, McCarroll SA, Medland SE, Miller KA, Montgomery GW,
433 Morrison AC, Muller-Nurasyid M, Navarro P, Nelis M, O'Connell JR, O'Donnell
434 CJ, Ong KK, Newman AB, Peters A, Polasek O, Pouta A, Pramstaller PP, Psaty
435 BM, Rao DC, Ring SM, Rossin EJ, Rudan D, Sanna S, Scott RA, Sehmi JS, Sharp
436 S, Shin JT, Singleton AB, Smith AV, Soranzo N, Spector TD, Stewart C,
437 Stringham HM, Tarasov KV, Uitterlinden AG, Vandenput L, Hwang SJ,
438 Whitfield JB, Wijmenga C, Wild SH, Willemsen G, Wilson JF, Witteman JC,
439 Wong A, Wong Q, Jamshidi Y, Zitting P, Boer JM, Boomsma DI, Borecki IB, van
440 Duijn CM, Ekelund U, Forouhi NG, Froguel P, Hingorani A, Ingelsson E,
441 Kivimaki M, Kronmal RA, Kuh D, Lind L, Martin NG, Oostra BA, Pedersen NL,
442 Quertermous T, Rotter JI, van der Schouw YT, Verschuren WM, Walker M,
443 Albanes D, Arnar DO, Assimes TL, Bandinelli S, Boehnke M, de Boer RA,
444 Bouchard C, Caulfield WL, Chambers JC, Curhan G, Cusi D, Eriksson J,
445 Ferrucci L, van Gilst WH, Glorioso N, de GJ, Groop L, Gyllensten U, Hsueh WC,
446 Hu FB, Huikuri HV, Hunter DJ, Iribarren C, Isomaa B, Jarvelin MR, Jula A,

- 447 **Kahonen M, Kiemenev LA, van der Klauw MM, Kooner JS, Kraft P, Iacoviello L,**
448 **Lehtimäki T, Lokki ML, Mitchell BD, Navis G, Nieminen MS, Ohlsson C, Poulter**
449 **NR, Qi L, Raitakari OT, Rimm EB, Rioux JD, Rizzi F, Rudan I, Salomaa V, Sever**
450 **PS, Shields DC, Shuldiner AR, Sinisalo J, Stanton AV, Stolk RP, Strachan DP,**
451 **Tardif JC, Thorsteinsdóttir U, Tuomilehto J, van Veldhuisen DJ, Virtamo J,**
452 **Viikari J, Vollenweider P, Waeber G, Widen E, Cho YS, Olsen JV, Visscher PM,**
453 **Willer C, Franke L, Erdmann J, Thompson JR, Pfeufer A, Sotoodehnia N,**
454 **Newton-Cheh C and Ellinor PT.** Identification of heart rate-associated loci and their
455 effects on cardiac conduction and rhythm disorders. *Nat Genet* 45: 621-631, 2013.
- 456 11. **Hibino H, Inanobe A, Furutani K, Murakami S, Findlay I and Kurachi Y.**
457 Inwardly rectifying potassium channels: their structure, function, and physiological
458 roles. *Physiol Rev* 90: 291-366, 2010.
- 459 12. **Hirose M, Carlson MD and Laurita KR.** Cellular mechanisms of vagally mediated
460 atrial tachyarrhythmia in isolated arterially perfused canine right atria. *J Cardiovasc*
461 *Electrophysiol* 13: 918-926, 2002.
- 462 13. **Hirose M, Leatmanorath Z, Laurita KR and Carlson MD.** Partial vagal denervation
463 increases vulnerability to vagally induced atrial fibrillation. *J Cardiovasc*
464 *Electrophysiol* 13: 1272-1279, 2002.
- 465 14. **Huang CL, Slesinger PA, Casey PJ, Jan YN and Jan LY.** Evidence that direct
466 binding of G beta gamma to the GIRK1 G protein-gated inwardly rectifying K⁺ channel
467 is important for channel activation. *Neuron* 15: 1133-1143, 1995.

- 468 15. **Ivanina T, Varon D, Peleg S, Rishal I, Porozov Y, Dessauer CW, Keren-Raifman T**
469 **and Dascal N.** Galphai1 and Galphai3 differentially interact with, and regulate, the G
470 protein-activated K⁺ channel. *J Biol Chem* 279: 17260-17268, 2004.
- 471 16. **Jiang M, Spicher K, Boulay G, Martin-Requero A, Dye CA, Rudolph U and**
472 **Birnbaumer L.** Mouse gene knockout and knockin strategies in application to alpha
473 subunits of Gi/Go family of G proteins. *Methods Enzymol* 344: 277-298, 2002.
- 474 17. **Kahr PC, Piccini I, Fabritz L, Greber B, Scholer H, Scheld HH, Hoffmeier A,**
475 **Brown NA and Kirchhof P.** Systematic analysis of gene expression differences
476 between left and right atria in different mouse strains and in human atrial tissue. *PLoS*
477 *One* 6: e26389, 2011.
- 478 18. **Kovoor P, Wickman K, Maguire CT, Pu W, Gehrmann J, Berul CI and Clapham**
479 **DE.** Evaluation of the role of I(KACh) in atrial fibrillation using a mouse knockout
480 model. *J Am Coll Cardiol* 37: 2136-2143, 2001.
- 481 19. **Krapivinsky G, Gordon EA, Wickman K, Velimirovic B, Krapivinsky L and**
482 **Clapham DE.** The G-protein-gated atrial K⁺ channel IKACH is a heteromultimer of
483 two inwardly rectifying K(+) -channel proteins. *Nature* 374: 135-141, 1995.
- 484 20. **Lakatta EG, Maltsev VA and Vinogradova TM.** A coupled SYSTEM of intracellular
485 Ca²⁺ clocks and surface membrane voltage clocks controls the timekeeping mechanism
486 of the heart's pacemaker. *Circ Res* 106: 659-673, 2010.

- 487 21. **Leaney JL, Milligan G and Tinker A.** The G protein α subunit has a key role in
488 determining the specificity of coupling to, but not the activation of G protein-gated
489 inwardly rectifying K^+ channels. *J Biol Chem* 275: 921-929, 2000.
- 490 22. **Leaney JL and Tinker A.** The role of members of the pertussis toxin-sensitive family
491 of G proteins in coupling receptors to the activation of the G protein-gated inwardly
492 rectifying potassium channel. *Proc Natl Acad Sci U S A* 97: 5651-5656, 2000.
- 493 23. **Li N, Csepe TA, Hansen BJ, Sul LV, Kalyanasundaram A, Zakharkin SO, Zhao J,**
494 **Guha A, Van Wagoner DR, Kilic A, Mohler PJ, Janssen PM, Biesiadecki BJ,**
495 **Hummel JD, Weiss R and Fedorov VV.** Adenosine-Induced Atrial Fibrillation:
496 Localized Reentrant Drivers in Lateral Right Atria due to Heterogeneous Expression of
497 Adenosine A1 Receptors and GIRK4 Subunits in the Human Heart. *Circulation* 134:
498 486-498, 2016.
- 499 24. **Liu GX, Derst C, Schlichthorl G, Heinen S, Seebohm G, Bruggemann A, Kummer**
500 **W, Veh RW, Daut J and Preisig-Muller R.** Comparison of cloned Kir2 channels with
501 native inward rectifier K^+ channels from guinea-pig cardiomyocytes. *J Physiol* 532:
502 115-126, 2001.
- 503 25. **Logothetis DE, Kurachi Y, Galper J, Neer EJ and Clapham DE.** The beta gamma
504 subunits of GTP-binding proteins activate the muscarinic K^+ channel in heart. *Nature*
505 325: 321-326, 1987.
- 506 26. **Lomax AE, Rose RA and Giles WR.** Electrophysiological evidence for a gradient of
507 G protein-gated K^+ current in adult mouse atria. *Br J Pharmacol* 140: 576-584, 2003.

- 508 27. **Luscher C and Slesinger PA.** Emerging roles for G protein-gated inwardly rectifying
509 potassium (GIRK) channels in health and disease. *Nat Rev Neurosci* 11: 301-315, 2010.
- 510 28. **Machhada A, Ang R, Ackland GL, Ninkina N, Buchman VL, Lythgoe MF, Trapp**
511 **S, Tinker A, Marina N and Gourine AV.** Control of ventricular excitability by
512 neurons of the dorsal motor nucleus of the vagus nerve. *Heart Rhythm* 12: 2285-2293,
513 2015.
- 514 29. **Mangoni ME, Traboulsie A, Leoni AL, Couette B, Marger L, Le QK, Kupfer E,**
515 **Cohen-Solal A, Vilar J, Shin HS, Escande D, Charpentier F, Nargeot J and Lory**
516 **P.** Bradycardia and slowing of the atrioventricular conduction in mice lacking
517 CaV3.1/alpha1G T-type calcium channels. *Circ Res* 98: 1422-1430, 2006.
- 518 30. **Mesirca P, Marger L, Toyoda F, Rizzetto R, Audoubert M, Dubel S, Torrente AG,**
519 **Difrancesco ML, Muller JC, Leoni AL, Couette B, Nargeot J, Clapham DE,**
520 **Wickman K and Mangoni ME.** The G-protein-gated K⁺ channel, IKACH, is required
521 for regulation of pacemaker activity and recovery of resting heart rate after sympathetic
522 stimulation. *J Gen Physiol* 142: 113-126, 2013.
- 523 31. **Nobles M, Sebastian S and Tinker A.** HL-1 cells express an inwardly rectifying K⁺
524 current activated via muscarinic receptors comparable to that in mouse atrial myocytes.
525 *Pflugers Arch* 460: 99-108, 2010.
- 526 32. **Nygren A, Lomax AE and Giles WR.** Heterogeneity of action potential durations in
527 isolated mouse left and right atria recorded using voltage-sensitive dye mapping. *Am J*
528 *Physiol Heart Circ Physiol* 287: H2634-H2643, 2004.

- 529 33. **Opel A, Nobles M, Montaigne D, Finlay M, Anderson N, Breckenridge R and**
530 **Tinker A.** Absence of the Regulator of G-protein Signaling, RGS4, Predisposes to
531 Atrial Fibrillation and Is Associated with Abnormal Calcium Handling. *J Biol Chem*
532 290: 19233-19244, 2015.
- 533 34. **Peleg S, Varon D, Ivanina T, Dessauer CW and Dascal N.** G(alpha)(i) controls the
534 gating of the G protein-activated K(+) channel, GIRK. *Neuron* 33: 87-99, 2002.
- 535 35. **Pfaffinger PJ, Martin JM, Hunter DD, Nathanson NM and Hille B.** GTP-binding
536 proteins couple cardiac muscarinic receptors to a K channel. *Nature* 317: 536-538,
537 1985.
- 538 36. **Posokhova E, Ng D, Opel A, Masuho I, Tinker A, Biesecker LG, Wickman K and**
539 **Martemyanov KA.** Essential role of the m2R-RGS6-IKACH pathway in controlling
540 intrinsic heart rate variability. *PLoS One* 8: e76973, 2013.
- 541 37. **Riven I, Iwanir S and Reuveny E.** GIRK channel activation involves a local
542 rearrangement of a preformed G protein channel complex. *Neuron* 51: 561-573, 2006.
- 543 38. **Riven I, Kalmanzon E, Segev L and Reuveny E.** Conformational rearrangements
544 associated with the gating of the G protein-coupled potassium channel revealed by
545 FRET microscopy. *Neuron* 38: 225-235, 2003.
- 546 39. **Sakmann B, Noma A and Trautwein W.** Acetylcholine activation of single
547 muscarinic K+ channels in isolated pacemaker cells of the mammalian heart. *Nature*
548 303: 250-253, 1983.

- 549 40. **Sarmast F, Kolli A, Zaitsev A, Parisian K, Dhamoon AS, Guha PK, Warren M,**
550 **Anumonwo JM, Taffet SM, Berenfeld O and Jalife J.** Cholinergic atrial fibrillation:
551 I(K,ACh) gradients determine unequal left/right atrial frequencies and rotor dynamics.
552 *Cardiovasc Res* 59: 863-873, 2003.
- 553 41. **Sebastian S, Ang R, Abramowitz J, Weinstein LS, Chen M, Ludwig A,**
554 **Birnbaumer L and Tinker A.** The in-vivo regulation of heart rate in the murine
555 sinoatrial node by stimulatory and inhibitory heterotrimeric G-proteins. *Am J Physiol*
556 *Regul Integr Comp Physiol* 305: 435-442, 2013.
- 557 42. **Slesinger PA, Reuveny E, Jan YN and Jan LY.** Identification of structural elements
558 involved in G protein gating of the GIRK1 potassium channel. *Neuron* 15: 1145-1156,
559 1995.
- 560 43. **Wickman K, Nemej J, Gendler SJ and Clapham DE.** Abnormal heart rate regulation
561 in GIRK4 knockout mice. *Neuron* 20: 103-114, 1998.
- 562 44. **Wickman KD, Iniguez Lluhl JA, Davenport PA, Taussig R, Krapivinsky GB,**
563 **Linder ME, Gilman AG and Clapham DE.** Recombinant G-protein beta gamma-
564 subunits activate the muscarinic-gated atrial potassium channel. *Nature* 368: 255-257,
565 1994.
- 566 45. **Zaritsky JJ, Redell JB, Tempel BL and Schwarz TL.** The consequences of
567 disrupting cardiac inwardly rectifying K(+) current (I(K1)) as revealed by the targeted
568 deletion of the murine Kir2.1 and Kir2.2 genes. *J Physiol* 533: 697-710, 2001.

569 46. **Zuberi Z, Birnbaumer L and Tinker A.** The role of inhibitory heterotrimeric G-
570 proteins in the control of in-vivo heart rate dynamics. *Am J Physiol Regul Integr Comp*
571 *Physiol* 295: R1822-R1830, 2008.

572 47. **Zuberi Z, Nobles M, Sebastian S, Dyson A, Shiang Y, Breckenridge RA,**
573 **Birnbaumer L and Tinker A.** Absence of the inhibitory G-protein, $G\alpha_{i2}$, predisposes
574 to ventricular cardiac arrhythmia. *Circ Arrhythm Electrophysiol* 3: 391-400, 2010.

575

576

577

578 **Table Legends**

579

580 **Table 1. Deletion of $G\alpha_{i2}$ or $G\alpha_{i1/3}$ and GIRK currents kinetics across the atria.** Cells
581 were clamped at -60 mV and carbachol was applied for 20 ms with a fast perfusion system.
582 Characteristics of the GIRK currents kinetics are presented in the table for the LA, RA and
583 SAN region for the $G\alpha_{i2}$ (+/+) (n= 10-12 from 4 mice), $G\alpha_{i2}$ (-/-) (n= 8-10 from 5 mice), and
584 $G\alpha_{i1/3}$ (-/-) (n=5-8 from 3 mice). The current inactivation characteristics (τ_{deac} and lag inac)
585 were faster in the RA and SAN compared to the LA (*p<0.05).

586

587 **Table 2. Quantitative real-time reverse transcription PCR to measure gene expression**
588 **in the RA and LA.** Quantitative real-time reverse transcription PCR was performed as
589 described in the Materials and Methods for the genes indicated in the Table. Measurements
590 were performed in triplicate from $G\alpha_{i2}$ (-/-) mice (n=3 mice) and littermate controls (n=3
591 mice) (*p<0.05 using one way ANOVA).

592

593 **Figure Legends**

594

595 **Figure 1. GIRK currents in the atrial tissue.** A. Representative traces of currents measured
596 in atrial myocytes isolated from the left and right atria of $G\alpha_{i2}$ (+/+) mice. B. Mean current-
597 voltage relationships. Atrial myocytes were challenged with 10 μ M carbachol. GIRK currents
598 were larger in RA compared to LA (n=10 from 6 mice).

599

600 **Figure 2. Deletion of $G\alpha_{i2}$ affect the gradient of GIRK across the atria.** Representative
601 traces and mean current-voltage relationships of currents measured in atrial myocytes isolated
602 from the left and right atria of $G\alpha_{i2}$ (-/-) mice. Basal GIRK currents were larger in RA
603 compared to $G\alpha_{i2}$ (+/+) (n=5-6 from 4 mice).

604

605 **Figure 3. Deletion of $G\alpha_{i1/3}$ affect the gradient of GIRK across the atria.** Representative
606 traces and mean current-voltage relationships of currents measured in atrial myocytes isolated
607 from the left and right atria of $G\alpha_{i1/3}$ (-/-) mice. There was a loss of GIRK current gradient
608 between the LA and RA (n=7-8 from 4 mice).

609

610 **Figure 4. Comparison of GIRK currents in the LA and RA.** Bar graph showing maximum
611 GIRK currents measured at -120 mV. In $G\alpha_{i2}$ (+/+), carbachol (10 μ M) led to a larger
612 activation of GIRK currents in the RA (n= 10 from 6 mice). Deletion of $G\alpha_{i2}$ led to larger
613 basal and carbachol-activated currents in the RA (n=6 from 4 mice). Deletion of $G\alpha_{i1/3}$ led to
614 smaller carbachol-activated currents in both LA and RA with a marked effect in the RA (n=8
615 from 4 mice), the consequence being a loss of gradient across the atria.

616

617 **Figure 5. GIRK current in the SAN.** Left panel: Representative traces of GIRK currents in
618 control and after activation with 10 μ M carbachol. Comparison is made between $G\alpha_{i2}$ (+/+)
619 (n=18 from 8 mice), $G\alpha_{i2}$ (-/-) (n=15 from 5 mice) and $G\alpha_{i1/3}$ (-/-) (n=16 from 7 mice). Right
620 panel: Mean current-voltage relationships. Atrial myocytes were challenged with 10 μ M
621 carbachol. GIRK currents were not affected by $G\alpha_i$ deletion.

622

623 **Figure 6. Consequence of the deletion of $G\alpha_{i2}$ on the action potential of single**
624 **cardiomyocytes.** Single cardiomyocytes AP were measured after stimulation of cells by a 5
625 ms pulse after pacing at 1Hz for 60 seconds. In $G\alpha_{i2}$ (+/+) the APD90 were longer in the RA
626 (n=8-9 from 3 mice), although the mean values did not reach significance when analyses with
627 t-test due to the variability of the data values. In $G\alpha_{i2}$ (-/-) (n=6-7 from 3 mice), both APD50
628 and APD90 were significantly reduced in the right atria (* p<0.05).

629

630 **Figure 7. Electrophysiology of isolated right and left atria.** A) Atrial effective refractory
631 period (ERP), (B) conduction velocity (CV) and (C) minimum wave front cycle length
632 (mWFCL) in left atrial tissue deficient in $G\alpha_{i2}$ (-/-) mice compared to $G\alpha_{i2}$ (+/+) (* p-value
633 <0.05). Dose-response for carbachol on left atrial AERP (D), relative AERP to baseline (E)
634 and CV (F) in $G\alpha_{i2}$ (-/-) mice compared to $G\alpha_{i2}$ (+/+). Experiments were performed with 7
635 mice in each group.

636

637

Table 1

	Gαi2 (+/+)			Gαi2 (-/-)			Gαi1/3 (-/-)		
	LA	RA	SAN	LA	RA	SAN	LA	RA	SAN
	<i>N</i> = 9	<i>N</i> = 8	<i>N</i> = 10	<i>N</i> = 12	<i>N</i> = 10	<i>N</i> = 11	<i>N</i> = 7	<i>N</i> = 8	<i>N</i> = 5
Im, pA/pF	-85 ± 8	-86.5 ± 7.8	-55.9 ± 8	-77.6 ± 6.2	-75.1 ± 7	-49.7 ± 6.2	-67 ± 4.2	-70 ± 9.5	-58.2 ± 18
GIRK, pA/pF	-106 ± 15	-162 ± 34.5	-108.3 ± 20	-87.8 ± 8.2	-128 ± 12	-118.3 ± 14.4	-92.51 ± 10	-134.8 ± 24	-175.2 ± 18
Lag + TTP, s	1.06 ± 0.06	0.84 ± 0.05	0.99 ± 0.01	0.9 ± 0.05	0.82 ± 0.04	0.96 ± 0.05	1 ± 0.05	0.68 ± 0.04	0.79 ± 0.07
tac, ms	188 ± 11.1	142 ± 11.3	162 ± 24.4	156 ± 10.8	153 ± 27	144 ± 7.2	256 ± 45	114 ± 13	143 ± 13.7
tdeac, ms	2996 ± 458	811 ± 66.6*	607 ± 92*	2654 ± 438	779 ± 137*	466 ± 40.3*	3567 ± 739	824 ± 141*	493 ± 71.3*
lag inac, s	0.68 ± 0.14	0.32 ± 0.06*	0.21 ± 0.01*	0.59 ± 0.08	0.33 ± 0.03*	0.23 ± 0.02*	0.53 ± 0.01	0.30 ± 0.07*	0.26 ± 0.01*
% des 20 s	25.8 ± 2.35	25.2 ± 3.34	20 ± 1.5	29.5 ± 3.4	27.1 ± 2.9	31 ± 3.2	22.5 ± 1.6	24.1 ± 2.7	14.1 ± 3.5
G	22.7 ± 1.3	18.7 ± 1	26.4 ± 2.7	25 ± 2.2	19.6 ± 1.3	22.8 ± 2.4	34.4 ± 3.3	22.6 ± 2.6	17.8 ± 2.2

Table 2

Genes	WT	KO	WT	KO
	LA	LA	RA	RA
	Δ CT	Δ CT	Δ CT	Δ CT
Gnai1	6.75 \pm 0.06	6.98 \pm 0.05	8.46 \pm 0.35	8.15 \pm 0.09
Gnai3	6.90 \pm 0.18	6.65 \pm 0.08	6.98 \pm 0.12	7.42 \pm 0.09
Gnb1	4.76 \pm 0.14	5.72 \pm 0.25*	5.21 \pm 0.50	5.50 \pm 0.07
Gnb4	7.98 \pm 0.18	7.72 \pm 0.07	8.75 \pm 0.18	8.60 \pm 0.08
Gng7	10.8 \pm 0.14	11.5 \pm 0.14	11.5 \pm 0.51	11.7 \pm 0.16
Gng11	7.04 \pm 0.11	7.49 \pm 0.03*	7.56 \pm 0.21	7.43 \pm 0.04
Kcnj3	2.86 \pm 0.14	2.30 \pm 0.07	3.62 \pm 0.18	3.00 \pm 0.05
Kcnj5	5.38 \pm 0.12	4.86 \pm 0.06*	5.51 \pm 0.24	4.94 \pm 0.07*

Figure 1

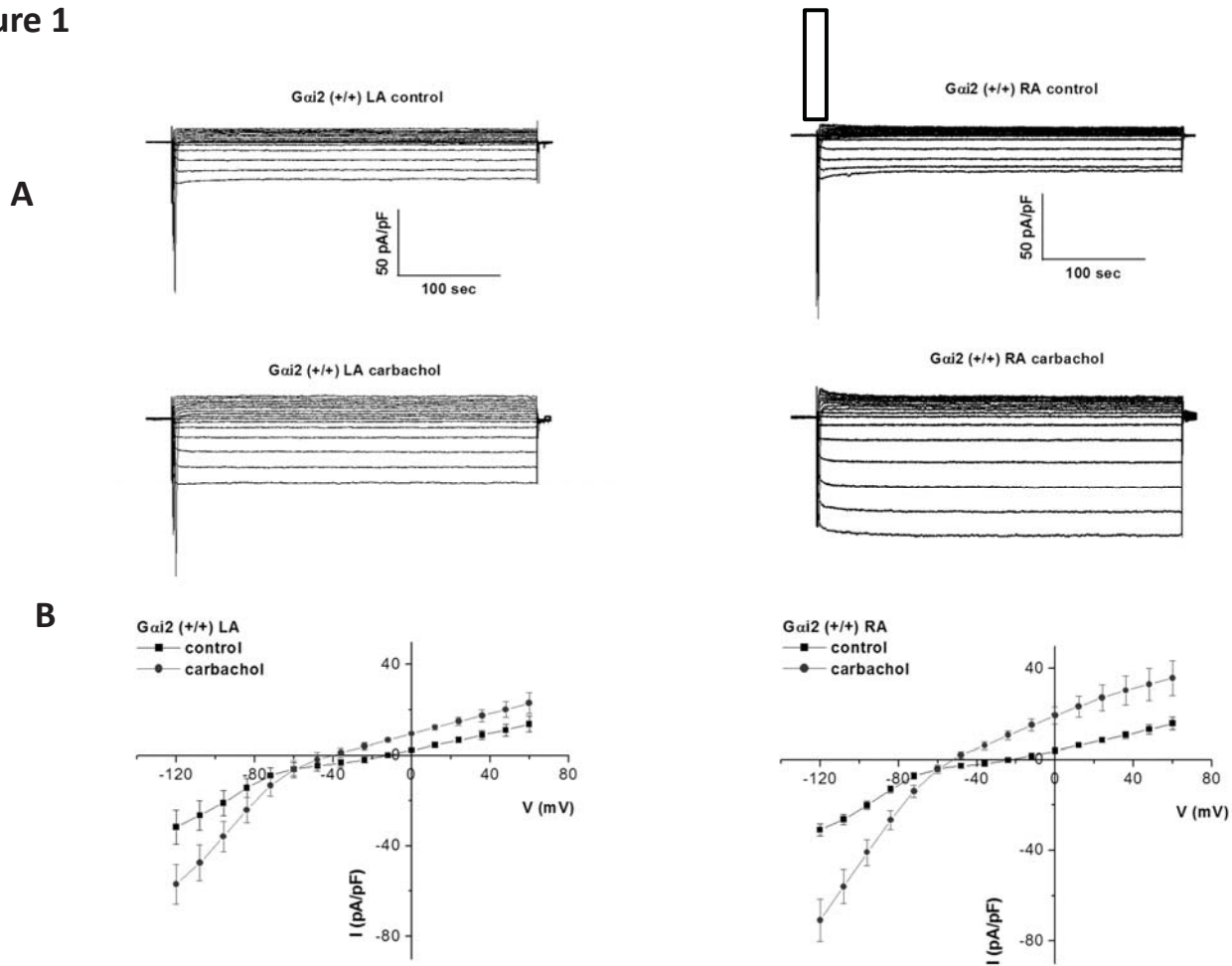


Figure 2

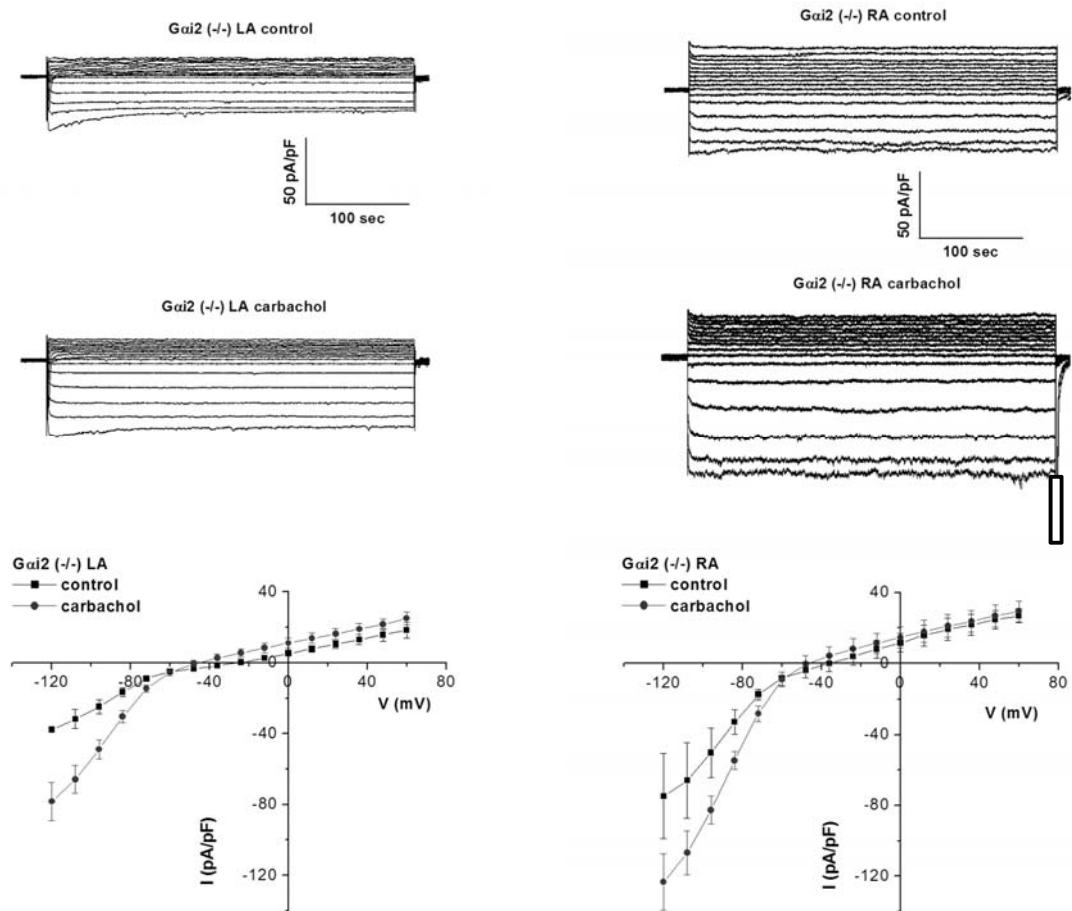


Figure 3

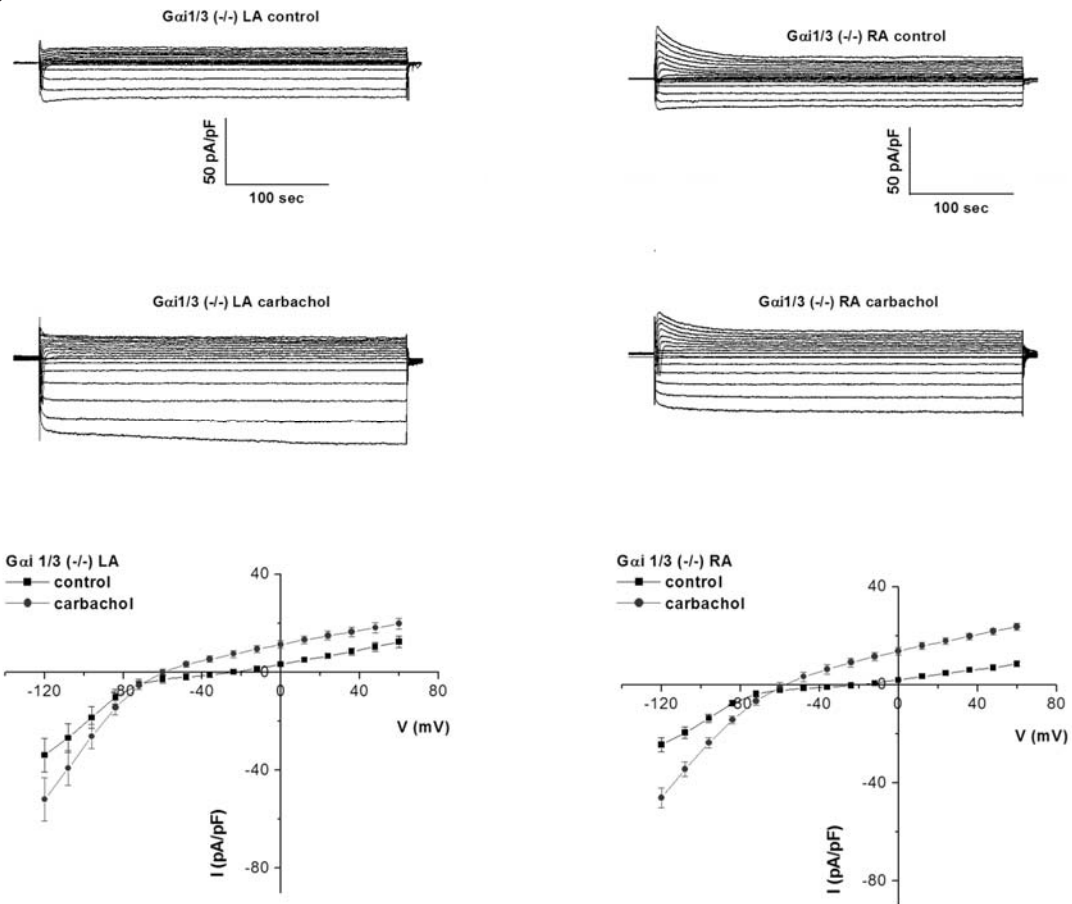


Figure 4

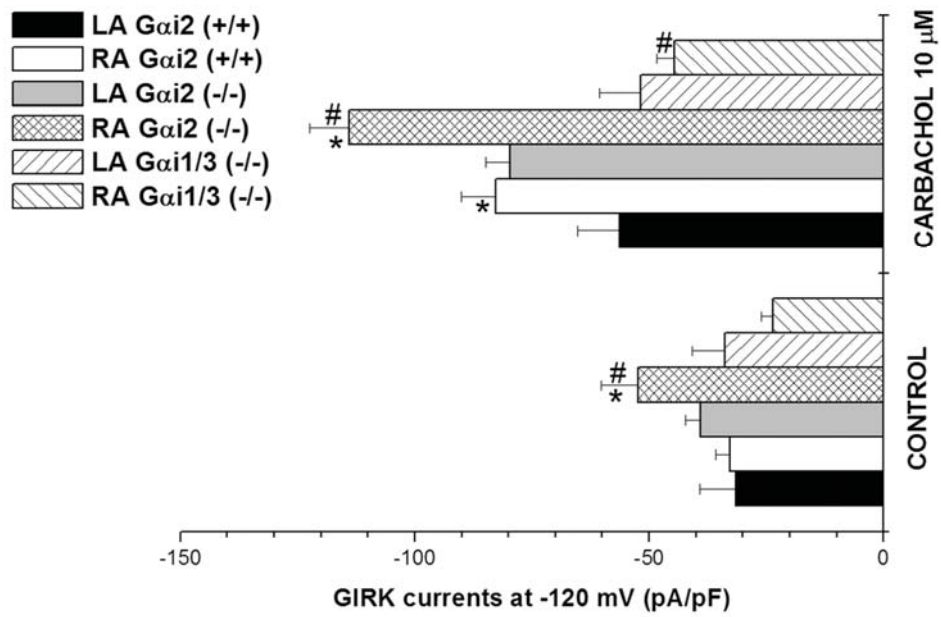


Figure 5

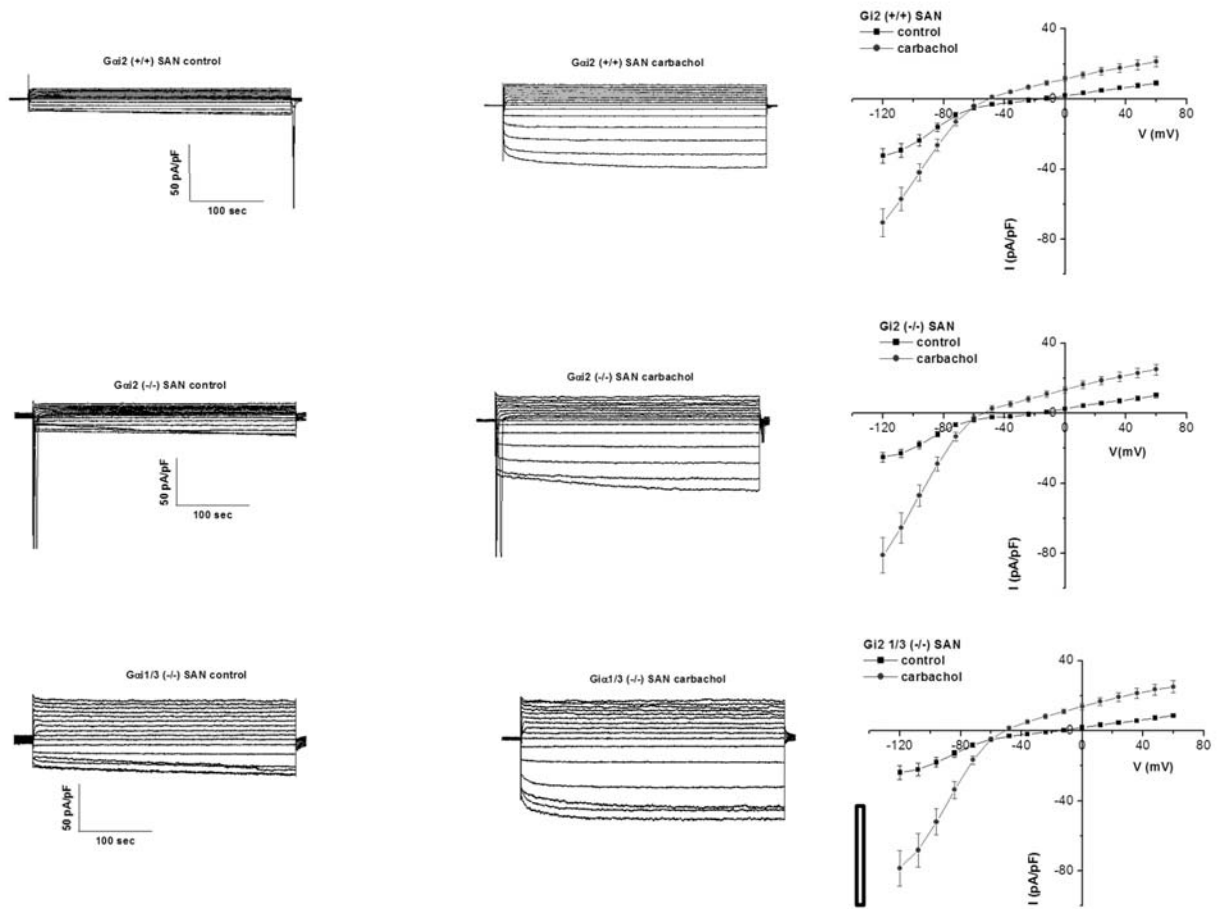


Figure 6

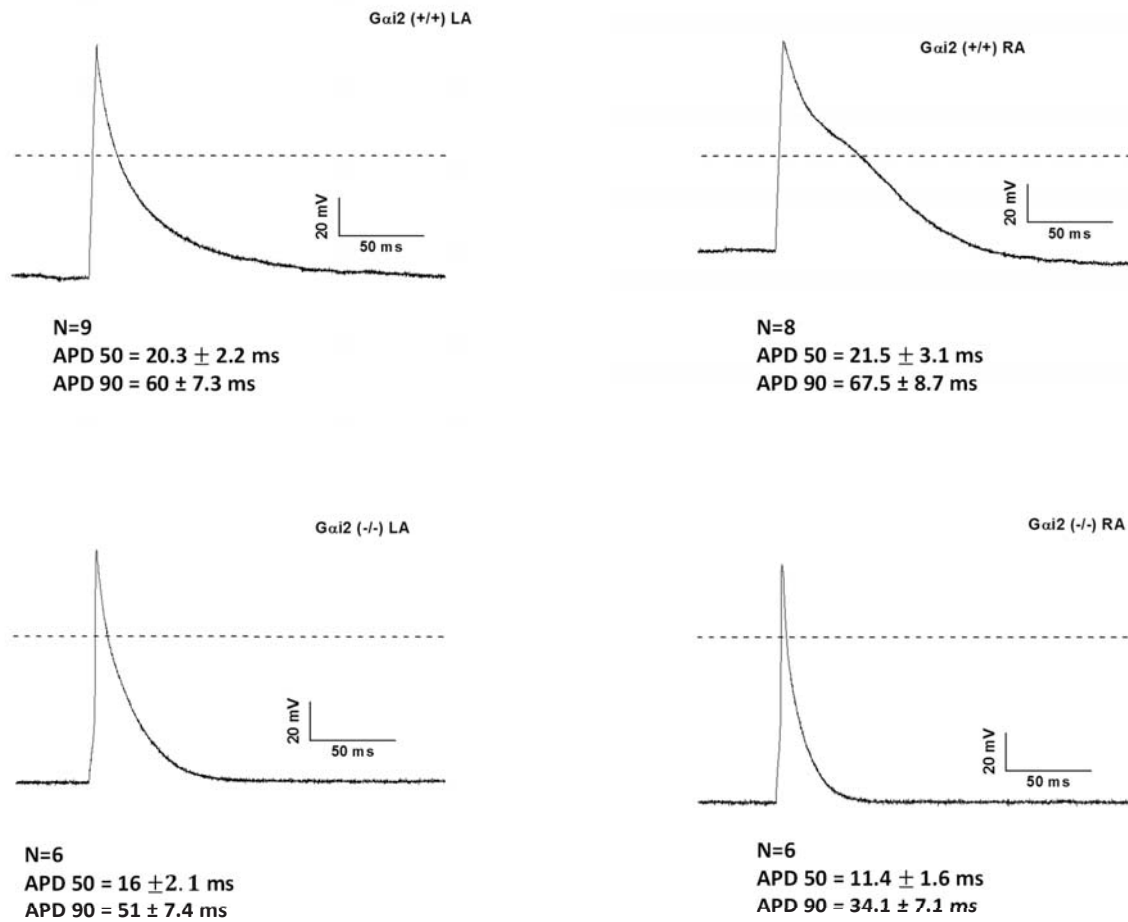


Figure 7

